He^0 on D_2 collisions at keV energies and the HeH_2 energy surface

John Jakacky, Jr., Edward Pollack, Ralph Snyder, and Arnold Russek
Department of Physics, The University of Connecticut, Storrs, Connecticut 06268
(Received 18 June 1984)

An experimental and theoretical study of He^0 on D_2 collisions at energies 1.0, 1.5, and 2.0 keV has been carried out to probe and to understand the energy surface of the ground electronic state of the HeH_2 triatomic molecule and of the intersections of this surface with those of low-lying electronically excited states. At each collision energy, doubly differential energy-loss spectra have been obtained and the results have been analyzed in terms of a parametric fit to an *ab initio* calculated ground-state energy surface. The scaled energy loss for quasielastic collisions (electronically elastic collisions with vibrational-rotational excitation) are shown to constitute a sensitive probe of the region of the ground-state energy surface in which the proximity of the He projectile breaks the H_2 (or D_2) bond. Sigmund scaling has been experimentally demonstrated to hold for the quasielastic channel in He on D_2 collisions despite the strong presence of electronically inelastic processes, a finding of particular significance, since the scaling law was derived under the assumption that there are no accessible electronically inelastic channels in the collision system. The theoretical study confirms this behavior for collisions in which electronic excitation is velocity independent and occurs in well-defined surface intersection regions. Cross sections differential in angle but integrated over all vibrotational-rotational inelastic energy losses have been both calculated and experimentally measured for the quasielastic channel, and the two are found to be in good agreement.

I. INTRODUCTION

The successful work of recent decades on atom-atom collisions is now being extended to include atom-molecule systems. Although collisions involving molecular targets are more difficult to address, studies carried out in the last few years have already shown clear progress toward understanding the basic principles involved in electronic excitation which occurs in atom-molecule collisions. In this context we cite the recent work of Dowek *et al.*[1] on the direct and exchange scattering in the He^+ and He^0 on H_2 collisions. Earlier studies[2] on $He^+ + H_2$ showed that the cross sections for electronic excitation and the initial interpretation of the results are quite similar to what had been found in the ion-atom cases. As an example, the similarity between collisions of He^+ or He^0 with H_2 and with He targets is particularly striking.[1] In the energy range of these studies, atom-molecule collisions generally show a dominance of the electronically elastic channel at the smallest scattering angles with the electronically inelastic channels dominating at the larger angles. Atom-molecule scattering involving only the ground electronic state which results in vibro-rotational excitation is termed "quasielastic." The quasielastic channel is of particular interest, since it yields information on the ground-state potential-energy surface, the important surface for most chemical reactions.

In this paper, we report on quasielastic scattering as well as on some aspects of the electronically inelastic scattering in He^0 on D_2. The present study is an extension of our earlier work on Ne^+ and Ne^0 collisions with H_2 and D_2.[3] The work on neon confirmed the applicability of the Sigmund scaling law[4] for f, the most probable scaled energy loss in a quasielastic collision. The law predicts that in collisions between atoms and diatomic molecules, when no electronically inelastic channels are present, a scaled most probable energy loss f, where $f=(M_D/M_{He})(\Delta E/E\theta^2)$ for He on D_2 collisions, is a function only of $\tau=E\theta$, where E is the collision energy and ΔE the most probable energy lost by the projectile in the laboratory frame. This scaling law was verified[3] in the Ne^+ and Ne^0 cases, where the inelastic channels are very weak. Indeed, the $Ne^+ + H_2$ and D_2 collisions were selected to fulfill this condition.

In the $He^0 + D_2$ system we find[5] (in agreement with the recent results of Dowek *et al.*[1]) that the electronically inelastic channels are strong in the τ range investigated. They are in fact dominant at $E=1.5$ keV for $\tau > 1.5$ keV deg. Nevertheless, the experimental results demonstrate the applicability of the energy-loss scaling in the entire τ range studied. The most probable scaled energy loss for the electronically elastic channel is seen to be a function of τ only. This is found even in the large-τ range where the quasielastic channel is weak, despite the fact that one of the assumptions in the Sigmund derivation of the scaling law requires the electronically elastic channel to be the only open channel.

Recently *ab initio* calculations have been made for the HeH_2 ground-state energy surface.[6] It has become apparent[7] that studies of low-keV energy collisions of He on H_2 yield valuable information about this surface. A theoretical study, based on this energy surface, is presented and interpreted. The results of this study are shown to be in agreement with the experimentally determined most probable energy-loss values. In addition, the calculated differential cross sections for the quasielastic channel are seen to be in reasonable agreement with the experimental results.

II. EXPERIMENTAL TECHNIQUES AND RESULTS

The experimental arrangement used for the $He^0 + D_2$ measurements is shown in Fig. 1. He^+ is generated in an ion source (a), extracted, and focused by an einzel lens (b, c, d). The He^+ beam passes through a set of horizontal and vertical shim fields and a collimating hole into a beam "chopping" region (g) consisting of two plates (about 1 cm long and separated by 0.5 cm). One of the plates is maintained at a fixed bias while the other has a voltage pulse ($=18$ V, 0.1 μsec wide, and at a frequency of 100 kHz) impressed upon it. The He^+ beam passes through additional shim fields into a Wien filter for velocity analysis (j), and into a charge-exchange cell (k) where it is partially neutralized. The combined He^+ and He^0 pass through sweep plates (l) where the remaining He^+ ions are deflected. The He^0 beam enters the scattering cell containing D_2 (or He) target gas and scatters through an angle θ into the detector chamber. The scattered He^0 beam passes through an electrostatic energy analyzer (not used in the present study) into a drift tube to a detector (q). The detector is similar in design to one previously described.[8] The beam strikes and ejects electrons from a circular metal "detecting" surface. The electric fields in the detector are adjusted to direct the ejected electrons into a channeltron. The resulting pulse is amplified, passed through a constant fraction discriminator and serves as a start pulse for a time-to-amplitude converter. The stop pulse to the converter is provided by the chopping voltage pulse which is suitably delayed. The basic techniques for time-of-flight measurements are discussed in Ref. 9. For cross-section measurements an automated system is used to control a stepping motor for changing angles. The data are recorded by a multichannel analyzer.

The incident beam is collimated by two circular apertures. The first of these (13 mils in diameter; 1 mil $\equiv 10^{-3}$ in.) serves as the exit aperture on the charge-exchange cell, and the second (18 mils) as the entrance to the scattering cell. The scattered beam passes through a third hole (15 mils) serving as an exit hole for the scattering cell. It passes through a fourth before entering the entrance slit (effective width 2 mils) of the electrostatic energy analyzer. The He^0 is detected by a metal surface (0.5 in. in diameter). In this set of measurements the angular resolution is primarily determined by hole 3 and the diameter of the detecting surface. As is generally the case, the measured resolution is better than that given by the geometrical definition. In these measurements the full width at half maximum (FWHM) of the detected beam is typically less than 0.1 deg.

In a small-angle collision the scattering angle is given by $\theta = \Delta p/p$, where Δp is the momentum transfer to the target and p is the momentum of the incident particle.[3] For an incident particle of energy E and mass M_p scattered *elastically* by a target of mass M_t, the energy lost by the projectile, ΔE, will be denoted in this special case by T, given by $T = \Delta p^2/2M_t = (M_p/M_t)E\theta^2$. In the case of an atomic target, the projectile energy loss in elastic collisions is well defined at a given scattering angle. Because of energy transferred to vibrational-rotational degrees of freedom, scattering from a molecular target results in a projectile energy-loss distribution which depends on the molecular orientation, internuclear separation, and on the impact parameters that result in scattering into the angle θ. At each angle the difference between the measured energy loss ΔE and the elastic energy loss T represents Q, the vibro-rotational excitation energy of the target. A scaling law, derived by Sigmund,[4,10] predicts that in the case of a homonuclear diatomic target molecule, a quantity f, defined by $f = 0.5(1 + Q/T)$, is a function only of τ. The scaling law was derived under the assumption that the collision is electronically elastic. Figure 2 presents the results for the peaks in the f versus τ distributions for 1.5-keV He^0 on D_2 collisions in a plot of ΔE versus $E\theta^2$. The ΔE values are determined at each angle by comparing the location of the quasielastic peak in the He^0 on D_2 collisions to that of the elastic peak in He^0 on He collisions. Scattering from He yields data which lie on the elastic curve, since the He targets have no vibrational-rotational degrees of freedom. Fully elastic scattering from D_2, which has the same mass as He, would result in data lying along the same elastic curve. For $E\theta^2 > 4$ keV deg^2, the data lie above the elastic curve; the displacement in ΔE above the elastic limit gives the vibrational-rotational excitation energy Q.

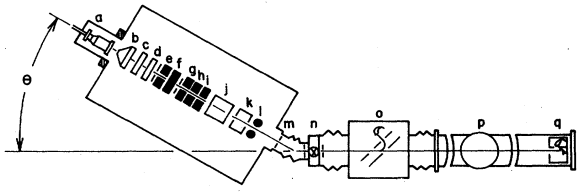

FIG. 1. A schematic of the experimental arrangement. Ion source (a), extractor and einzel lens system (b, c, d), deflector plates (e through i), Wien filter (j), charge-exchange cell (k), deflector plates (l), scattering cell (m), valve (n), electrostatic energy analyzer (o), cryo-pump (p) and time-of-flight (TOF) detector (q). The distance from the scattering cell to the TOF detector is 4.2 m.

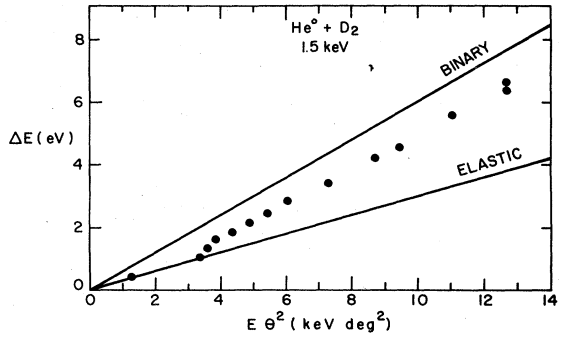

FIG. 2. The quasielastic energy loss (ΔE) vs $E\theta^2$ for $He^0 + D_2$ at 1.5 keV. The binary and elastic limits are represented by the two lines shown. The difference, in eV, between the data and the elastic curve represents the vibro-rotational excitation Q.

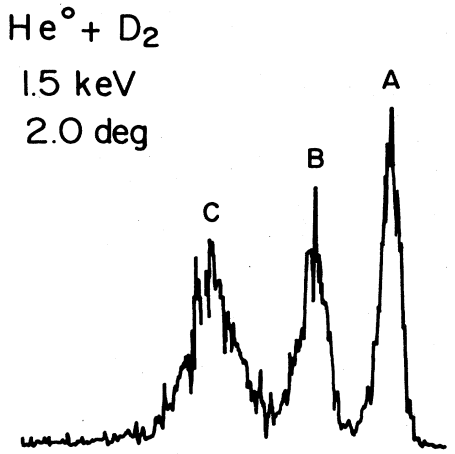

FIG. 3. Typical spectrum for $He^0 + D_2$ at 1.5 keV and 2.0 deg. Peak A is the quasielastic channel and peaks B and C are due to single and double electronic excitation channels, respectively. The energy separation between the maxima of peaks A and B is 14 eV and it is 35 eV between peaks A and C.

Although the theory primarily addresses collisions in the electronically elastic channel, this channel is in fact found to be weak over much of the τ range studied. Figure 3 shows a typical energy-loss spectrum at $E=1.5$ keV and $\theta=2.0$ deg. The peak labeled A is the electronically elastic channel, while peaks B and C involve electronically inelastic processes including excitation of the target and/or the projectile. These inelastic processes were discussed in detail in Ref. 1. Our results are in basic agreement with this earlier work. Figures 4, 5, and 6 present cross sections, differential in angle, for the processes corresponding to peaks A, B, and C at three energies. It may be clearly seen that the inelastic channels are dominant at the larger τ values. These cross sections are absolute and are obtained by comparison with the $He^0 + He$ cross sections at 0.5 deg for each energy. The $He^0 + He$ cross sections are obtained from an empirical potential.[11]

The results of our measurements on the electronically elastic channel are plotted in Fig. 7. The figure shows f versus τ at energies of 1.0, 1.5, and 2.0 keV, and confirms the scaling since the data can be well fit by a single curve. An essential point is now established: the scaling is valid for the electronically elastic channel in $He^0 + D_2$ even in the presence of strong inelastic collision processes.

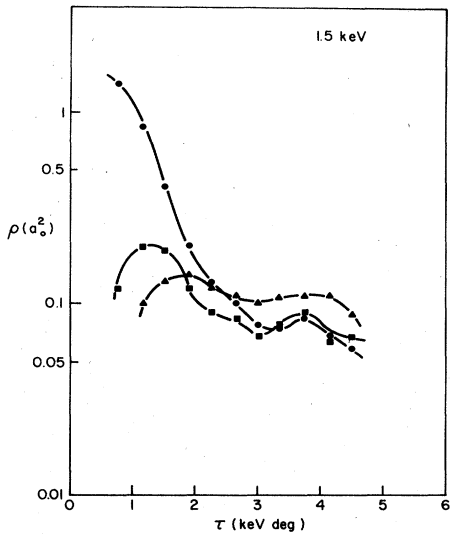

FIG. 5. The reduced cross sections at 1.5 keV. See caption for Fig. 4.

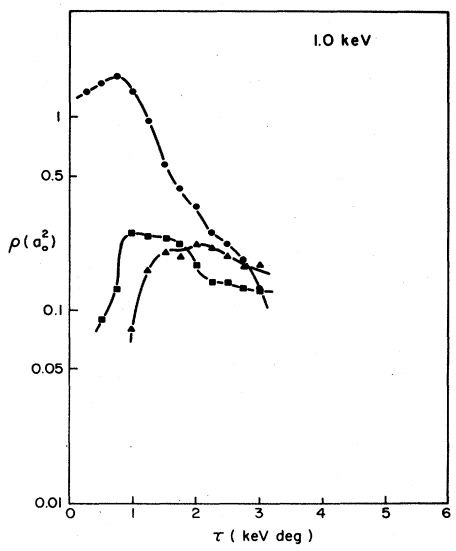

FIG. 4. The reduced cross sections [for peaks A (●), B (■), and C (▲)] vs the reduced scattering angle τ at 1.0 keV.

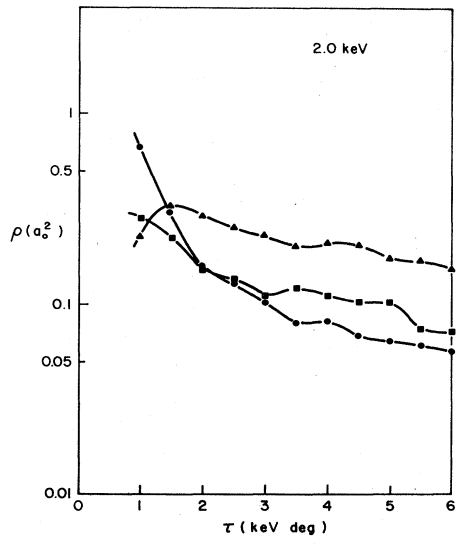

FIG. 6. The reduced cross sections at 2.0 keV. See caption for Fig. 4.

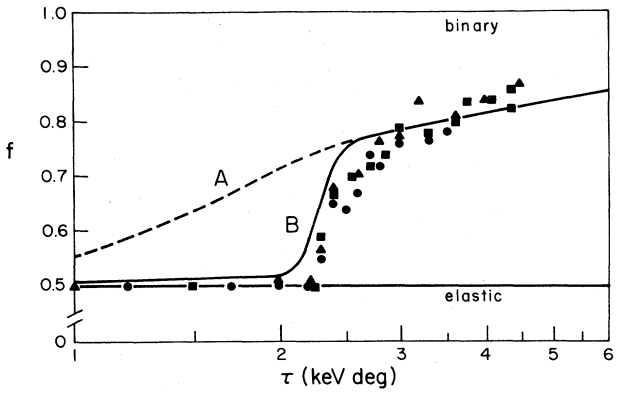

FIG. 7. A plot of the scaled energy loss f vs the reduced scattering angle τ for $He^0 + D_2$ collisions. The experimental results at 1.0 (●), 1.5 (■), and 2.0 (▲) keV are seen to follow a common curve, even though electronic excitation is strong in these collisions. The solid curve B shows the present theoretical calculations, using as interaction potential the parametric fit Eq. (1) with the correction term given by Eq. (4). The dashed curve A shows the earlier calculations of Ref. 12, which used Eq. (1) only.

III. THEORY

Two earlier papers[6,12] have laid the foundation for the theoretical studies to be reported here. In Ref. 6, Hartree-Fock calculations were carried out on the HeH_2 triatomic system which, combined with earlier studies at larger He-H_2 separation, determined most of the ground-state energy surface relevant to low-keV collisions. To facilitate scattering calculations using the energy surface, it is expressed in terms of a sum of Bohr and Born-Mayer terms whose deflection functions are convenient analytic functions. The *ab initio* calculations of the ground-state He-H_2 interaction energy surface was found to be rather well fit by a function of the form[6]

$$V(R,r,\gamma)=Z_p\left[\frac{e^{-\lambda_c R_A}}{R_A}+\frac{e^{-\lambda_c R_B}}{R_B}\right]+A_2\left[e^{-\lambda_p R_A}+e^{-\lambda_p R_B}\right]+A_3 e^{-\lambda_p R}-Be^{-bR}\,. \quad (1)$$

Z_p is the nuclear charge of the projectile and r is the H_2 internuclear separation. R_A and R_B are the distances from hydrogen atom A and B, respectively, to the helium atom. R is the distance from the helium atom to the center of the molecule and γ is the angle between $\mathbf{R}$ and $\mathbf{r}$. For the geometry of this system, see Fig. 1 of Ref. 6. The values of the parameters which best fit the parametric form (1) to the *ab initio* calculations are $Z_p=2$, $\lambda_c=3.20$, $A_2=1.20$, $\lambda_p=1.742$, $A_3=2.76$, $B=2.18$, and $b=2.2$. The total energy for the triatomic molecular system is then given by

$$E(R,r,\gamma)=V(R,r,\gamma)+E_{He}+E_{H_2}(r)\,. \quad (2)$$

The first two pairs of terms in V are two-body terms, the Bohr and Born-Mayer potentials, respectively. These are both taken over from atomic collision theory and give rise to vector additive forces along the directions $\mathbf{R}_A$ and $\mathbf{R}_B$. The Bohr terms describe screened Coulomb core-core repulsive forces. They are characteristically short range and are found to give the dominant contribution to vibro-rotational excitation. The Born-Mayer terms are characteristically longer in range than the screened Coulomb core-core terms and essentially describe Pauli-exclusion-principle polarization forces. They are due to the effect of antisymmetrization when the electronic wave functions overlap. The two-body Born-Mayer terms also contribute to vibro-rotational excitation; however, this contribution is small compared with that of the Bohr terms.

The third term in V is a long-range three-body term attributable to the interaction of the He with the excess electronic distribution between the two protons of the H_2 caused by the bonding σ orbitals. The fourth and final term is short range and provides saturation for the third as $R\rightarrow 0$. These latter two terms are three-body terms; they cannot be decomposed into pairs of forces that lie *along* $\mathbf{R}_A$ and $\mathbf{R}_B$. (Note that although any force can be decomposed into pairs of forces *parallel* to $\mathbf{R}_A$ and $\mathbf{R}_B$, it is an entirely different matter to decompose a force into a pair of forces *along* those vectors.) Any combination of two forces along $\mathbf{R}_A$ and $\mathbf{R}_B$ would result in forces internal to the molecule that would produce vibrational-rotational excitation. The three-body force due to the last two terms, the R-dependent terms, act on the molecule as a whole, as though it had no internal degrees of freedom. Being functions of R only, they act on the molecular center $R=0$, and therefore cannot contribute to vibro-rotational excitation. A detailed discussion is given by Snyder and Russek.[12]

The third term in Eq. (1) is necessary to describe the experimental f versus τ data. It was shown in Ref. 12 that a calculation of f versus τ using only the two-body Bohr term for the interaction between Ne^0 or Ne^+ with D_2 is on the binary limit for the entire τ range shown, whereas calculations for the same systems using the parametric form (1) have a significantly different behavior and fit the experimental data quite well.

Now that experimental results are available for He^0 on D_2, we extend the theory to allow quantitative comparisons of theory with experiment. In the remainder of this work, we (1) describe a modification of the parametric fit of the energy surface, given by Eqs. (1) and (2), (2) present a procedure for separating cross sections for electronically excited final states from that of the quasielastic channel, (3) compare the resulting calculated most probable f versus τ with the experimental values, and (4) calculate reduced differential electronically elastic cross sections $\rho(\tau)$ for comparison with the experimental results.

The particular functional form, Eq. (1), of the parametric fit to the self-consistent-field (SCF) calculation was chosen to facilitate the scattering calculations. The parameters were determined by adjusting them to fit the

Hartree-Fock energy calculations. Figure 2 of Ref. 6 already showed that this numerical fit was much less successful for $\gamma=90°$, although this discrepancy seemed small. However, a considerable discrepancy between the f versus τ values calculated with this parametric fit, curve A of Fig. 7, and the experimental values for He^0 on D_2 collisions has been traced to this small discrepancy at $\gamma=90°$. The total energy [see Eq. (2)] of the triatomic molecular system is shown in Figs. 8, 9, and 10 as a function of both r and R for $\gamma=90°$.

When comparing the total energies rather than only the He-H_2 interaction energies, it is necessary to add an additional r-dependent term, representing the energy of the isolated H_2 molecule, to the interaction energy V. This term is anharmonic and is well approximated by

$$E_{H_2}(r)=\frac{A}{r^m}-\frac{B}{r^n}+C\ , \tag{3}$$

where $A=0.650$, $B=0.779$, $C=3.830$, $m=2.2$, and $n=1.4$. The term C is an unimportant constant determined by our choice of the zero point of energy for the entire system. Even though Eq. (3) is not precise, it is good enough to study the effect of the incoming He on the H_2 bond. This term is not needed for fully impulsive collisions, for which there is a negligible displacement in r during the collision; it is needed only when studying the breakdown in impulsive behavior.

The comparison of the SCF calculation to the fit in this region of the energy surface, $\gamma=90°$, leads to two important conclusions. The first is that the shape of the fit has the same qualitative features as the SCF calculation. That is, as R is decreased, the potential well becomes shallower

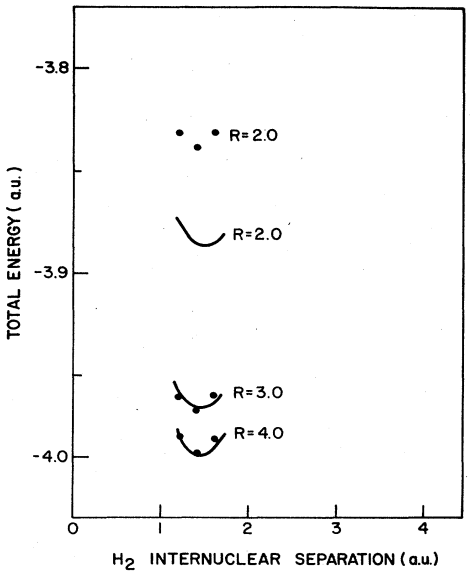

FIG. 8. The total energy of the HeH_2 triatomic system for different values of R, the atom-molecule separation, at $\gamma=90°$ vs r, the H_2 internuclear separation. The self-consistent-field (SCF) calculation is represented by the dots (●) and the potential fit by the curves.

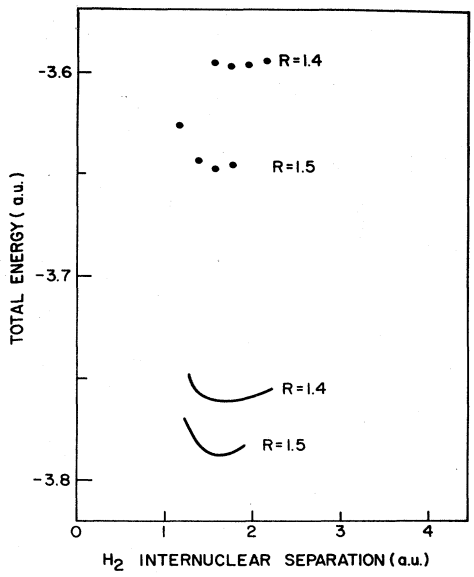

FIG. 9. See caption for Fig. 8.

but, the minimum in the r dependence remains fixed at $r=1.4$, moving out to larger values of r only when R decreases to 1.5 a.u., just before the minimum vanishes entirely, signaling a broken bond, at $R=1.3$. This broken bond is entirely a ground-electronic-state phenomenon, since surface intersections with excited electronic states do not occur until $R\leq 1.0$ a.u. The second conclusion is that a purely R-dependent term is missing from the parametric fit at $\gamma=90°$. Although the shapes of the r dependences in the parametric fit (see Figs. 8, 9, and 10) are correct, they must be shifted upward by an amount which varies with R. Thus, the discrepancy between the parametric fit and the *ab initio* calculations at $\gamma=90°$ can be removed

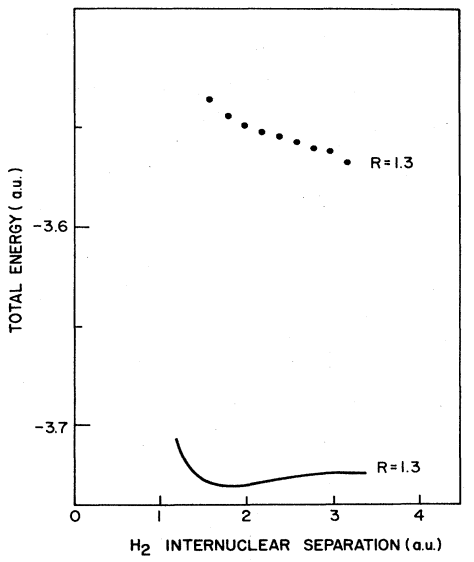

FIG. 10. See caption for Fig. 8.

by adding a repulsive R-dependent term:

$$V_{\text{corr}} = \begin{cases} 3.50e^{-2.15R} - 2.35e^{-3.20R} & \text{for } \gamma = 90° \\ \sim 0 \quad \text{for } \gamma \leq 60° . \end{cases} \tag{4}$$

which is good for $R > 0.5$ a.u. This is a correction term to Eq. (1) which has the effect of making a collision with $\gamma = 90°$ "harder" (a larger scattering angle for given impact parameter) and therefore has the effect of moving the "breakaway" point (the calculated τ value at which the data departs from the elastic curve) to a higher τ value. Furthermore, classical trajectory calculations show that the $\gamma = 90°$ case is dominant in determining the breakaway point.

In order to perform the scattering calculations to higher accuracy than is possible with the original parametric fit, Eq. (4) must be incorporated into the potential fit for cases involving large values of γ. Because of computer cost considerations, the correction is made by incorporating an algorithm into the computer code which decides which collision geometries are primarily small-γ cases for which the original parametric fit is adequate, and which collision geometries are primarily large-γ cases, for which the correction term (4) should be included. No tractable algorithm for this procedure will be exact because in general the projectile traverses a continuum of γ values as the collision evolves. However, as discussed below, the outcome of the collision calculations is very insensitive to the details of the algorithm used. Figure 11 shows the relevant geometry relating three angles: α, which gives the orientation angle of the molecule with respect to the target plane; the angle β defining the helium atom's position at closest approach; and Γ, the angle between the helium atom and the H_2 axis at that instant. Because the momentum exchange takes place predominantly near the point of closest approach, it is reasonable to choose Γ as the representative value of the general angle γ. Our method of incorporating Eq. (4) into the potential is to add it if and only if Γ is greater than 75° [halfway between 60° where Eq. (1) alone is sufficient and 90° where the correction Eq. (4) must be added to Eq. (1)]. To test

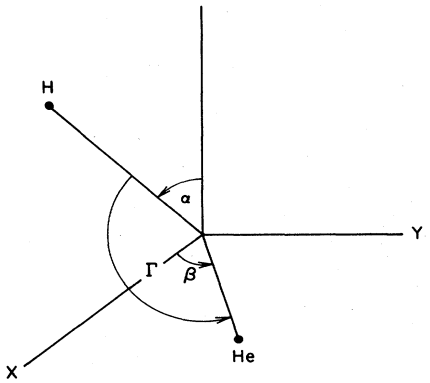

FIG. 11. Collision geometry. Here the z axis is parallel to the projectile velocity, as in Ref. 12. He indicates the point at which the helium projectile crosses the x-y target plane and H indicates the location of a target hydrogen atom in the x-z plane.

the sensitivity of this choice, we have investigated several other algorithms: some based on different critical values of Γ, and some based on β rather than Γ as the decisive angle. One of these algorithms mixes in the effects of Eq. (4) smoothly and continuously in the region of $60° < \Gamma < 90°$. These algorithms were used in a program described in Ref. 12 which uses the classical impulse approximation to calculate $f(\tau)$. The salient result is that the $f(\tau)$ predictions were nearly the same for all of these algorithms.

These algorithms should not be considered as models of the collision process. In principle, all collision calculations should be performed allowing the three nuclei to move according to Newton's laws under the influence of the forces which arise from the *ab initio* calculations, and indeed we have carried out some such calculations for $\gamma = 90°$. The results are given in Table I and discussed below. However, the cost of doing the 10^5–10^6 such classical trajectory calculations needed to give reasonable statistics for doubly differential cross sections is prohibitive. On the other hand, the cost of calculations using combinations of Bohr and Born-Mayer potentials, as in Eq. (1), is negligible, but the results are flawed for collision geometries which significantly probe the $\gamma = 90°$ region of the energy surface. Hence we have provisionally chosen the compromise outlined above, which is complicated to describe but computationally effective. The resulting f versus τ is shown as the solid curve B of Fig. 7, while the results which follow from Eq. (1) alone, without the correction term Eq. (4), are shown as the dashed curve A.

In order to obtain a preliminary insight into the breakdown of Sigmund scaling at low collision energies due to the beginning of adiabatic relaxation for the nuclear motion, we have carried out complete classical trajectory calculations for the $\gamma = 90°$ orientation of the HeD_2 triatomic system using Eqs. (1)–(4) for the total interaction energy and allowing all three nuclei to move. These calculations yield scattering angles (θ) and projectile energy losses (ΔE) for the energies (E) given in Table I. From this data f, at a particular orientation of the triatomic system ($\gamma = 90°$), was calculated and these results are also in Table I. Although $f(\gamma = 90°)$ only changes by a small amount for E between 3000 and 100 eV, a breakdown of the scaling of τ can be seen to begin between 100 and 200 eV.

TABLE I. Results of a classical scattering calculation of He^0 on D_2 for a fixed impact parameter ($b = 1.0$ bohr) and fixed γ ($= 90°$). The quantity f remains a good scaled variable down to 100 eV collision energy, but τ as a scaled variable breaks down at about 200 eV.

E (eV)	ΔE (eV)	θ (deg)	τ (keV deg)	$f(\gamma = 90°)$
3000	0.50	0.72	2.15	0.54
2000	0.75	1.07	2.14	0.54
1500	0.99	1.43	2.14	0.54
1000	1.47	2.12	2.12	0.54
500	2.82	4.18	2.09	0.53
200	6.17	9.85	1.97	0.52
100	9.56	17.7	1.77	0.52

The high-energy limit of Sigmund scaling is determined by breakdown in adiabatic behavior of the electronic motion, as evidenced by the onset of electronic excitation. This high-energy limit is impact-parameter (τ) dependent. The classical calculations described in Ref. 12 must be amended to remove the effects of the electronic excitation at larger values of τ. In the first instance, we perform this removal in a model in which it is assumed that if the projectile's impact parameter (distance of closest approach) is within the range of R such that electronically excited states are energetically available, it will have a statistically determined probability of being removed from the quasielastic channel. Since it is found experimentally that there are three main peaks in the $He^0 + D_2$ spectra with approximately equal probabilities for large τ, we have initially chosen the probability of removal to be two-thirds.[1] On the basis of Hartree-Fock studies of the type reported above[6] we choose $R_c = 1.0$ a.u. as the value of the critical radius for the region of electronic excitation. Figure 12 shows the surface intersections at $\gamma = 90°$ and $r = 1.4$ a.u. The angular dependence of one of these surface intersections is shown in Fig. 13. Although this model for removal of electronic excitation is a simple and very approximate one which may be improved upon in future work, it is sufficient in the angular region where the excitation is a small effect and serves *inter alia* to delineate that region. We note here the important point that removing electronic excitation in this simple way leaves the scaling property intact, that is, f remains a function of τ only for all projectile energies. For it is clear that the derivation of the scaling principle outlined in Ref. 12 is unaffected by present (projectile-energy independent) treatment of electronic excitation. So long as the probability for electronc excitation (and consequent removal from the quasielastic channel) is a function only of the impact parameters the projectile makes with the molecular target constituents and molecular center, the scaling laws continue to hold. All that is affected is the weights that close impacts contribute to the quasielastic f versus τ curve. Those impacts thus removed from the quasielastic f versus τ curve will reappear in f versus τ curves for electronically excited channels, which have not been studied in the present work. Thus we have obtained a loose but suggestive theoretical explanation of the experimentally observed fact that quasielastic scaling persists in the presence of electronically excited channels. Figures 4—6 suggest that a velocity dependence to the electronic excitation is just beginning to set in at 2 keV collision energy. Finally, we note that several central results of this work, including the calculated f versus τ, are largely independent of the excitation removal. Figure 7 shows the calculated f versus τ along with the experimental results. We note the close agreement of the two; Sec. IV of this paper discusses the comparison in more detail.

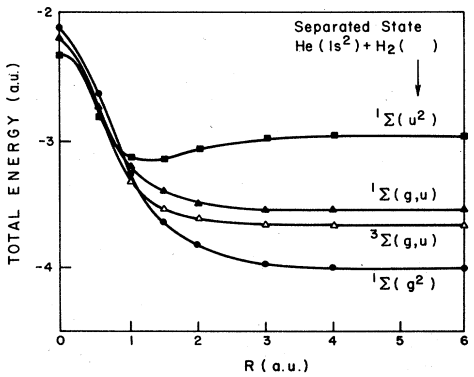

FIG. 12. Total energy of the HeH_2 triatomic system for $r = 1.4$ and $\gamma = 90$ deg vs R, the atom-molecule separation. Curve crossings between the ground electronic state $^1\Sigma_g^2$ and the three excited states are seen.

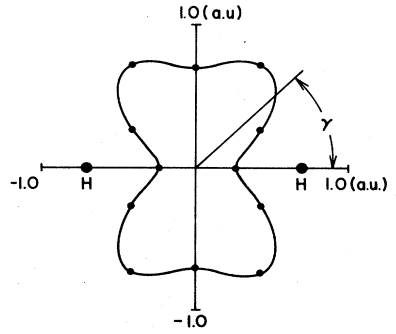

FIG. 13. Plot of R vs γ for the approximate surface intersections of the $He(1s^2) + H_2(^1\Sigma_g^2)$ state with that of $He(1s^2) + H_2(^1\Sigma_u^2)$.

In principle, the most desirable way to test the theory against experiment in this case would be a detailed comparison of the calculated doubly differential cross sections with the calibrated empirical energy-loss spectra. However, as discussed in Ref. 12, the experimental linewidths are at present dominated by instrumental effects, so such a complete test is not possible. The value of scaled energy loss, f, at which the distribution in f is maximum is one important parameter that can be obtained both experimentally and theoretically for confrontation of theory and experiment; this has been discussed above. Another such parameter is the reduced singly differential cross section to which we now turn:

$$\rho(\tau) = \sigma(\theta)\theta \sin\theta = \tau\sigma(\tau)/2\pi \, . \tag{5}$$

$\sigma(\tau)d\tau$ is the $\sin\alpha$ weighted area in the target plane (cf. Fig. 11) which leads to collisions between τ and $\tau + d\tau$. Equivalently it can be calculated by integrating the doubly differential cross section (whose calculation was described in Ref. 12) over all energy losses:

$$\sigma(\tau) = \int_{0.5}^{\infty} \sigma(\tau, f) df \, . \tag{6}$$

The program for calculating $\rho(\tau)$ was first tested with numerical calculations on several single-center potentials for which the exact result is known in closed form. These include Born-Mayer, Bohr (screened Coulomb), and

power-law potentials.[13] These studies indicate that convergence to accuracy levels of 1% or better occurs rapidly and uniformly. In order to probe the accuracy and reliability of the sampling of molecular orientations, other studies were made with simple two-center models in which a soluble one-center potential was associated with the position of each of the hydrogen atoms. In the limit of large τ, the exact $\rho(\tau)$ is thus known as twice the one-center result and provides a check on the numerical calculations. Here too the convergence and accuracy were satisfactory.

Figure 14 shows both the experimental and the theoretical $\rho(\tau)$. We wish to stress that the comparison is an absolute one; that is, the theoretical results are purely *ab initio* at low τ and the experimental measurements have been absolutely calibrated as described earlier. The comparison is most direct at low values of τ, where the theoretical calculations are independent of the absorbing sphere approximation. Encouragingly, the agreement is best in precisely that region.

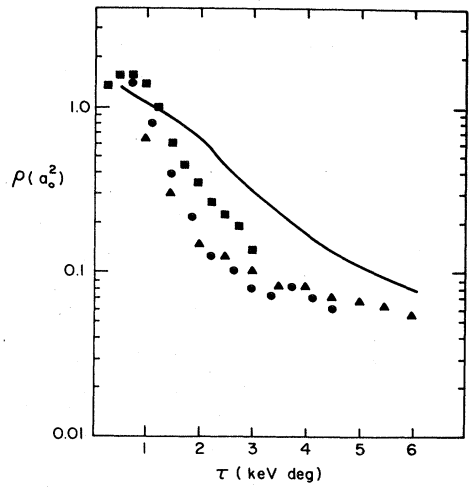

FIG. 14. Differential cross sections ρ as a function of the reduced scattering angle τ for quasielastic $He^0 + D_2$ collisions. The experimental points are given at 1.0 (■), 1.5 (●), and 2.0 (▲) keV. The agreement of the data taken at different projectile energies is generally consistent with the universal scaled $\rho(\tau)$. The solid curve represents the results of the theoretical calculations. The effects of electronic excitation on the theoretical quasielastic cross section are negligible for τ less than 1.5 keV deg.

IV. CONCLUSION

There is excellent agreement between the theoretical and experimental scaled-energy-loss function versus τ based on an *ab initio* energy surface. This is an indication that some understanding of the physics involved in the collision between an atom and a diatomic target has been attained. It is important to understand that a study of the f function is actually a study of the bond-breaking process.[14] As the projectile approaches close to the diatomic target during the collision, it exerts forces on the target. When the projectile—target-molecule distance becomes small enough, these forces momentarily break the bond between the H atoms. The bond then reforms as the projectile leaves the collision region, leaving the target molecule in a stable but vibrationally excited state. The f function is actually a measure of how much vibrational excitation the target has acquired as a function of τ, how deeply the projectile has penetrated into the molecular target.[14,15]

Another aspect to be considered is the sharpness of the breakaway of f from the elastic limit. This appears to be due to the sudden breaking of the bond in the molecular target. That is to say that virtually no vibrational excitation occurs until the projectile penetrates the molecule deeply enough to break the bond. This means that a certain R and therefore τ value must be reached before f can depart from the elastic limit.

The results for the differential cross sections are seen to be in good agreement with the experimental values over the entire range of τ. We reiterate the importance of the excellent agreement between theory and experiment at low values of τ, where the theoretical $\rho(\tau)$ are essentially independent of subsidiary assumptions about the electronically inelastic channels. We regard this agreement, which is within experimental uncertainties, as another successful link for atom-molecule and ion-molecule collision physics, where such direct confrontations of theory and experiment are rare.

Future work will focus on systems that do not scale,[15,16] although other work in this area will continue. Further theoretical and experimental studies are needed to understand the lack of scaling in some systems.

ACKNOWLEDGMENTS

This work was supported by the National Science Foundation under Grant No. PHY-83-03618 and by The University of Connecticut Research Foundation. We would like to acknowledge the contributions made by Dr. R. S. Peterson during the initial set-up period of the apparatus.

[1]D. Dowek, D. Dhuicq, V. Sidis, and M. Barat, Phys. Rev. A **26**, 746 (1982).

[2]A. V. Bray, D. S. Newman, and E. Pollack, Phys. Rev. A **15**, 2261 (1977).

[3]N. Andersen, M. Vedder, A. Russek, and E. Pollack, Phys. Rev. A **21**, 782 (1980).

[4]P. Sigmund, J. Phys. B **11**, L145 (1978).

[5]J. Jakacky, Jr., V. Heckman, and E. Pollack, in *Abstracts of the Thirteenth International Conference on the Physics of Electronic and Atomic Collisions, Berlin, 1983,* edited by J. Eichler, W. Fritsch, I. V. Hertel, N. Stolterfoht, and V. Wille (North-Holland, Amsterdam, 1983), p. 587.

[6]A. Russek and R. Garcia G., Phys. Rev. A **26**, 1924 (1982).
[7]J. Ioup and A. Russek, Phys. Rev. A **8**, 2898 (1973).
[8]W. L. Hodge, Jr., A. L. Goldberger, M. Vedder, and E. Pollack, Phys. Rev. A **16**, 2360 (1977).
[9]Q. C. Kessel, E. Pollack, and W. W. Smith, in *Collisional Spectroscopy,* edited by R. G. Cooks (Plenum, New York, 1977), Chap. 2.
[10]P. Sigmund, J. Phys. B **14**, L321 (1981).
[11]S. G. Lambrakos, Ph.D. thesis, Polytechnic Institute of New York, 1983 (unpublished).
[12]R. Snyder and A. Russek, Phys. Rev. A **26**, 1931 (1982).
[13]To avoid any possible ambiguity, we note that the reduced Rutherford cross section in our notation is given by $\rho(\tau)=A^2/\tau^2$ if $V(r)=A/r$.
[14]A. Russek, in *Electronic and Atomic Collisions,* edited by J. Eichler, I. V. Hertel, and N. Stolterfoht (Elsevier, Amsterdam, 1984), p. 701.
[15]J. Jakacky, Jr. and A. Russek, in *Abstracts of the Thirteenth International Conference on the Physics of Electronic and Atomic Collisions, Berlin, 1983,* edited by J. Eichler, W. Fritsch, I. V. Hertel, N. Stolterfoht, and U. Wille (North-Holland, Amsterdam, 1983), p. 614.
[16]M. Vedder, H. Hayden, and E. Pollack, Phys. Rev. A **23**, 2933 (1981).